Conference Proceedings

EuroSun 2016
Palma de Mallorca (Spain), 11 - 14 October 2016

A Comparison Study of Solar Thermal Collector Performance in the Tropics

Arifeen Wahed[1] and Thomas Reindl[1]

[1] Solar Energy Research Institute of Singapore, Singapore

Abstract

Over the recent years, awareness on integration of a solar thermal system for industrial process heating applications has been increased. In the Tropics, a huge potential on similar applications has been identified due to availability of abundant solar energy throughout the year. However, challenges lie on selection of an appropriate solar thermal collector for supplying required thermal energy to the industrial processes in tropical conditions with fluctuation irradiance and ambient high moisture air.

A test methodology has been developed in order to evaluate the solar thermal collector efficiency via measured data, a model based time resolved simulation analysis. In this analysis, collectors were tested at an outdoor test facility in the tropical condition. Collector model was developed and optimized the collector parameters for validating the experimental results. The validated collector model was then utilized to determine the efficiency parameters of the collector. Thus, the proposed method of comparing the collector performance would provide a valuable basis for selection of the appropriate collector technology to be utilized in a large-scale solar thermal system for industrial heating applications.

Keywords: *Solar thermal collector performance, tropics, industrial process heat.*

1. Introduction

Solar energy has emerged as a competitive source of energy compare to the conventional source of fossil energy due to concern of economic and environmental considerations. Utilization of solar thermal energy for industrial heating applications is one such targeted areas. At present, about two hundred large scale solar heating plants have been identified for industrial heating applications [SHIP] all around the world. Solar thermal collector is one of the key components of solar heating systems. Thus, selection of right type of solar thermal collector is crucial for industrial heating applications.

Collector thermal performance is generally tested either by steady-state test (SST) method or by quasi-dynamic test method. Researchers have been working on development of new and more effective test methods [Amer et al., 1997; Perers, 1997; Kratzenberg et al., 2006; Kong et al., 2012a, 2012b; Xu et al., 2012] that could predict the collector performance more accurately. In general, solar thermal collectors are certified by a specific test standard such as ISO 9806. This certificate provides the general basis for comparing different collector performances. However it is of particular interest to compare different collector performance for a particular condition such as the tropical climatic conditions in Singapore, where fluctuation irradiation and high humidity exists. The present study of the collector performance is thus not to redefine the existing test methods; rather to develop a test methodology for comparing the collector performance by outdoor testing over a period of time in the tropical climate. Thus the proposed study provides input for selection of the right type solar thermal collector, which is very much important for industrial heating applications.

In this study, solar thermal collectors' outdoor performance has been tested; and an evacuated model based on time resolved simulation has been developed to evaluate the collector thermal performance from the dynamic test performances. This method is an effective way of comparing collector outdoor thermal performance in the

Selection and/or peer review under responsibility of Scientific Committee
doi:10.18086/eurosun.2016.06.02 Available at http://proceedings.ises.org

tropics, where a high fluctuation of irradiation has been observed.

2. Collector outdoor test

An experimental test facility, as shown in Fig. 1 of a solar thermal collector system has been installed at the roof top of the Solar Energy Research Institute of Singapore (SERIS).

Fig. 1: Solar Thermal collector testing system at the roof top of the Solar Energy Research Institute of Singapore (SERIS). Three different solar thermal collectors were installed for the test operation.

2.1. Experiments setup

For collector testing, three different collectors were setup in parallel. Other components of the test facility were a thermostat system including water tank, chiller, heater and temperature controller, three water flow pumps with variable speed drive for each collector, power control panel and data acquisition system. The testing collectors comprise of different technologies – (i) flat plate collector incorporated with evacuated technology, (ii) evacuated tube collector, and (iii) evacuated tube with heat-pipe technology. Testing area of each collector was approximately 4 to 5 m^2.

During experiments, the heat generated by these solar thermal collectors was discharged via the thermostat. The thermostat, controlled by the temperature controller via temperature sensors was heated up or cooled down the water in the storage tank, if required. Collector pre-set input water temperatures were supplied to the collectors from the storage tank. Water flow through each collector was controlled by the variable speed driven water pump. To measure water temperature and water flow, temperature sensors and water flowmeters were installed at the different positions of the system. A silicon sensor and a temperature sensor were installed to measure radiation and ambient temperature respectively. During test operation, data acquisition, processing and system control were achieved by utilizing the National Instrument systems through LabVIEW program.

For measurements, instruments such as (i) four-wire Class A type PT100 Resistance Temperature Detectors (RTD) for temperature measurement, (ii) magnetic flowmeters with low volumetric flow rate in the range of 0 to 1 $m^3.h^{-1}$ for flow measurement, (iii) silicon sensor (transducer set range 0 – 70 mV) for irradiance measurement and (iv) National Instrument (NI) equipment for control, data acquisition and processing were installed for test operation. A graphical user interface (GUI) of the solar thermal test system was developed in the LabVIEW for the purpose of the data processing, analyses and control with high flexibility. For data acquisition, one (1) second time resolution was set for all experiments.

Calibration of these sensors was performed in order to achieve a higher accuracy of the measured data. RTD temperature sensor, water flow meter and silicon sensors were calibrated before deployed for experiments. RTD (PT-100, 4-wire, Class A) sensors correction had been performed against a calibrated Platinum Resistance Thermometer (PRT). The magnetic flowmeter and the silicon sensor were also calibrated with a correction formula for higher accuracy. Even though the sensors were calibrated, there were systematic uncertainties in the systems. Tab. 1 lists the sensors' systematic uncertainties to be considered.

Tab. 1: Measuring sensors systematic uncertainties

Parameters	Sensor type	Range	Uncertainty
1. Temperature	RTD (PT-100, 4-wire, Class A)	0 to 200 ºC	0.02 ºC *
2. Water flow	Magnetic flowmeter (Rosemount 8732)	0 to 0.9 m^3/h	max. deviation ±0.025% of max. reading +
3. Solar irradiance	Silicon sensor (Mono-Si PV Cell)	0 to 1600 W/m^2	± 2.0% #
4. Data logging	NI analog input connector	4 to 20 mA	Gain error (reading): 0.76%

* Based on calibration report by A* Star Metrology Centre
\+ Flowmeter calibration test report by POLYCONTROLS
\# Test report – precision measurement of a PV irradiance sensor, Fraunhofer ISE

2.2. Test procedures

In order to determine the yield of the solar thermal collectors – in particular comparing the yield of different type of collectors in parallel against each other, an experimental test procedure, 'constant collector flow', had been followed. Under the experimental boundary conditions, collector flow was fixed but different minimum flow rates through each collector type according to the recommendation of the manufacturer. And the inlet temperature was same for all collectors during experiment and could be varied in the range of 80 to 100°C.

Tab. 2: Experiments conditions for fixed flow and constant inlet temperature for each collector

Collector	Irradiation, W/m^2	Ambient temperature, ºC	Water flow, m^3/h	Collector inlet water temperature, ºC		
Collector A	Ambient condition 100 - 1000	Ambient condition 30 - 34	0.10 – 0.12	80	90	~ 100
Collector B			0.17 - 0.20			
Collector C			0.13 – 0.16			

As observed from Tab. 2, the inlet water temperature boundary condition was relatively high during experiments, 80 to 100°C. Because the collectors were tested for industrial process heating application and such inlet water temperature range could represent the actual industrial process heating applications. Collector yield performance results were discussed in Section 4.2.

2.3. Stagnation test

In a tropical climate, supply of solar thermal heat may far exceed the heat demand due to the stagnation condition of the solar thermal system. This may raise the collector temperature above 200°C. Increasing stagnation temperature may lead to thermal stress of the collector. In order to determine the collector performance after such stagnation condition, tests were performed on the collectors.

For stagnation test, collector pumps were switched off and all three collectors were exposed to the ambient irradiance condition for continuously seven days. During this stagnation test, all the collector loops were filled with water.

After the stagnation test, a visual inspection had been performed to figure out any physical damage, wear and tear of the collectors including the corresponding joints. No visual defects including any wear and tear had been observed on these collectors. After visual inspection, experiments were performed with the same boundary conditions for all three collectors, as stated in the Tab. 2

3. Solar collector model

In order to evaluate the collector efficiency via measured data, model based time resolved simulation analyses have been developed. The method is well adapted to the fluctuating solar radiation conditions in the tropics. It allows for determining various collector parameters under non equilibrium conditions.

3.1. Collector mathematical model

During experiments three different technologies were investigated – (i) Collector A: flat plate vacuum solar thermal panel, (ii) Collector B: evacuated tube collector, and (iii) Collector C: evacuated tube collector with heat pipes. Even though these collectors use different technologies to absorb solar thermal heat, the mechanism of harnessing solar thermal heat is almost similar – evacuated technology and selective absorbers are used for all these collectors. In case of Collector A and Collector B, solar thermal heat is conducted by the absorbers directly to the collector fluid. In case of Collector C collector solar thermal heat is conducted indirectly to the collector fluid through heat pipe.

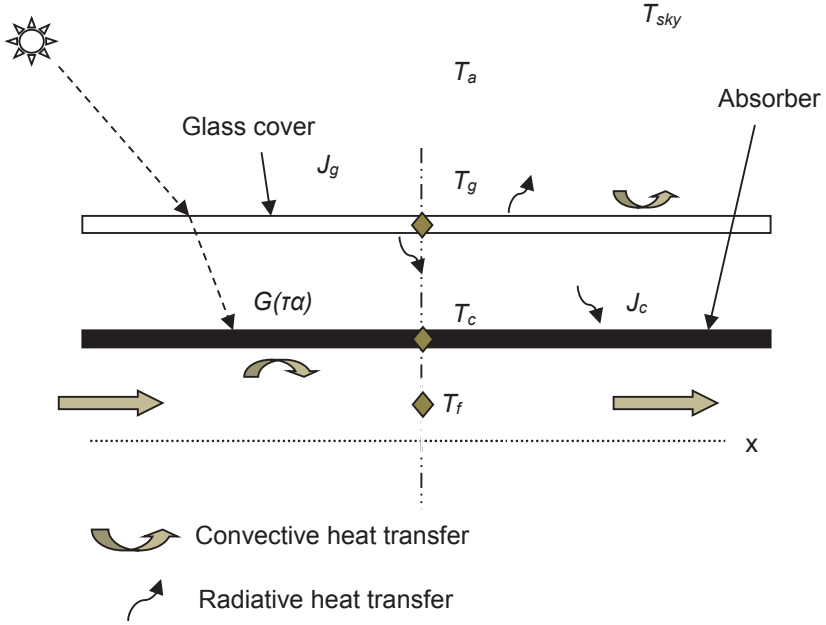

Fig. 2: Evacuated tube collector model. T_g, T_c, and T_f are the temperature of glass, absorber and fluid respectively. T_a is the ambient temperature and T_{sky} is the radiation temperature of the sky. G is the solar irradiance, α is the optical absorptance and τ is the transmittance coefficient. J_g and J_c are the heat capacity of glass and absorber respectively

An evacuated collector model as shown in Fig. 2 is considered to describe the different types of heat energy coupling between the absorber of the collector and the fluid applied for heat transfer. The assumption for these simplifications is the sufficiently accurate conformance between measured and modelled (simulated) time series of collector data, as shown in Section 4. Additional assumptions in the model are – (i) flow of the heat transfer fluid is unidirectional, along one axis (ii) properties of glass and absorber are independent of temperature (constant) (iii) thermo-physical properties of the water are temperature dependent (iv) no heat is supposed to be transported in the fluid moving direction by heat conduction (v) effect of the varying incidence angle of the solar radiation on the collector performance is neglected (vi) infrared emissivity of the sky is one (ε_{sky}=1).

As shown in Fig. 2, radiated heat transfer between the sky and the glass cover is taken into account. Heat transfer between the back cover and the ambient is assumed to be dominated by convection (radiative and conductive heat transfer is neglected here). Since there is almost no medium (vacuum) between the cover and the absorber, the heat transfer between these two components is assumed to be purely due to radiation.

Evacuated tube collector modelling is done following the publication of Praene et al. (2005). The model consists of 3 thermal nodes, namely, the transparent glass cover, the absorber plate and the heat transfer fluid. It is considered that the temperature of the fluid is a function of x (flow direction along x - axis) and the fluid is moving in an effective single channel with a velocity u (u=function of distance x, and time, t). Thus the thermal nodes can be expressed as,

For the transparent glass cover:

$$J_g \rho_g \frac{dT_g}{dt} = \varepsilon_g \sigma(T_{sky}^4 - T_g^4) + h_{g,a}(T_a - T_g) + \frac{\varepsilon_c \varepsilon_g}{\varepsilon_c + \varepsilon_g - \varepsilon_c \varepsilon_g} \sigma(T_c^4 - T_g^4) \quad \text{(eq. 1)}$$

The sky temperature of (eq. 2) can be obtained from the ambient temperature by using Swinbank's formula [Deacon, 1970],

$$T_{sky} = 0.0552 T_a \quad \text{(eq. 2)}$$

For the absorber plate:

$$J_c \rho_c \frac{dT_c}{dt} = G(\tau\alpha) + \frac{\varepsilon_c \varepsilon_g}{\varepsilon_c + \varepsilon_g - \varepsilon_c \varepsilon_g} \sigma(T_g^4 - T_c^4) + h_{f,c}(T_{fx,t} - T_c) \quad \text{(eq. 3)}$$

For the heat transfer fluid:

$$C_f \rho_f \frac{\pi d_{in}^2}{4} \left(\frac{dT_{f\,x,t}}{dt} + u \frac{dT_{f\,x,t}}{dx} \right) = \pi d_{in} h_{f,c}(T_c - T_{f\,x,t}) \quad \text{(eq.4)}$$

The collector heat removal channel is modelled as a single fluid channel, which is divided into N segments. The temperature values $T_f(x,t)$, $T_g(t)$ and $T_c(t)$ at every segment are obtained by solving the equations- (eq. 1), (eq.2), (eq.3) and (eq.4).

3.2. Collector parameter identification and model validation

Input parameters for identification in the model are (i) infrared emissivity of glass cover, (ii) glass heat capacity (specific heat of glass times glass thickness), (iii) absorber tube diameter, (iv) heat transfer co-efficient between glass and ambient, (v) heat transfer co-efficient between water and absorber, (vi) infrared emissivity of absorber, (vii) transmittance-absorptance co-efficient of the absorber, and (viii) absorber heat capacity (specific heat of absorber times absorber thickness). Tab.3 shows the input values obtained from data sheets (Engineering toolbox) and own assessment (Mahbubul 2013) for sensitivity analysis.

Tab. 3: Input parameter values for sensitivity analysis

Input parameter	Unit	Value
Collector absorber specific Heat capacity	J/kg K	400
Collector absorber thickness	m	0.001
Collector absorber emissivity	-	0.09
Collector absorber pipe diameter	m	0.0135
Heat transfer coefficient absorber-fluid	W/(m^2 K)	10
Transmittance-absorptance coefficient		0.86
Collector glass specific heat capacity	J/kg K	840
Collector glass thickness	m	0.0025
Collector glass emissivity	-	0.9
Heat transfer coefficient glass-air	W/(m^2 K)	9

The following steps are considered to identify the corresponding collector parameters in order to validate the model with experimental results (water is used as heat transfer fluid).

Step 1: Set the constant parameters (i) collector dimensions, (ii) collector glass and absorber densities, (iii) water properties as function of temperature, (water properties are determined for the mean fluid temperature T_m (average water temperature of collector inlet and collector outlet) at any time, using interpolation in the

water properties table.

Step 2: Input the experiment's data (time resolution one minute) into the model (i) mass flow rate, (ii) ambient temperature, (iii) irradiance, (iii) collector inlet water temperature.

Step 3: Perform sensitivity analysis of the identified parameters on the model (detailed discussion on the top of this section). Only the sensitive parameters – change of RMSE ≤ 1K with respect to the change of input parameter values in the range of ±10%, are considered for the optimization process. Else, input the parameter values (as constant) in the model.

Step 3a: In the optimization process, input an upper range value and a lower range value for each parameter selected for optimization. After optimization, input the optimized values to the model.

Step 4: Run the model. Compare the collector outlet temperature (simulated values) with the corresponding experimental values of the collector outlet temperature

Step 5: Calculate the root mean square (RMSE) of collector outlet temperature between the simulation value and the experiment value. Set the stopping criteria 10-6 K (a threshold to terminate the iteration when the successive iteration of the defined RMSE function does not satisfy the condition). This iteration process continues until the stopping criteria are satisfied.

Step 6: After optimization, the parameter values of the validated model are checked with another set of experimental data and step 4 and step 5 are repeated. If this condition is satisfied, the optimized parameters of the model are identified; else, repeat the procedures outlined in step 3a to step 6.

The parameter identification and model validation approach was adopted for three different collectors analysed – Collector A, Collector B and Collector C. The corresponding results obtained are discussed in the Section 4.2.

3.3. Collector efficiency parameter

In a dynamic model, the collector efficiency is defined as a ratio of the useful energy gain to the incident solar radiation power, as mentioned in (eq. 5),

$$\eta(t) = \frac{\dot{m} C_f(t)[T_o(x,t) - T_i(x,t)]}{G(t)A} \qquad \text{(eq. 5)}$$

The water temperature at the collector inlet, $T_i(x,t)$ and the collector outlet, $T_o(x,t)$ are obtained from the valid model, (eq. 4).

In a stationary model, the collector efficiency is usually defined as the function of collector efficiency parameters (η_0, a, and b) as mentioned in (eq. 6),

$$\eta = \eta_0 - a\frac{(T_m - T_a)}{G} - b\frac{(T_m - T_a)^2}{G} \qquad \text{(eq. 6)}$$

Collector validated dynamic efficiency model of (eq. 1) to (eq. 5) were used to determine the efficiency parameters η_0, a, and b of the stationary model from (eq. 6). By applying a multiple linear regression method on the simulation results these coefficients (η_0, a, and b) can be determined. The corresponding results for three different collectors – Collector A, Collector B and Collector C, are discussed in Section 4.2.

4. Results and discussions

Outdoor testing of the collectors was performed over a period of time. Collector experiment results were used to validate the collector models via fitted identified parameters. The collector models were then utilized to identify the efficiency parameters for collector performance analysis.

4.1. Outdoor test performance

According to the test procedures described in Section 2.2, experiments were performed for each of the three collector for three months. After that testing, a stagnation test as described in Section 2.3 followed by each collector performance test were performed.

During experiments, collector flows were maintained at the minimum flow condition recommended by the collector manufacturers as shown in Tab. 2. Minimum flow condition of the collector had been chosen to attain maximum temperature gain across the collectors. Since each collector technology has different specifications, minimum flow condition recommended by the manufacturer had been considered for experiments.

Thermal performances of the each collector, as shown in Fig. 3, were recorded by measuring the collector water temperature at the inlet and at the outlet. As observed from Fig. 3 collector inlet temperatures were maintained constant at ~80°C and the collector outlet temperature varies due to the fluctuation of irradiance during operation. Similar experiments with different collector inlet temperatures such as 90°C and ~100°C as described in Tab. 2, had also been performed.

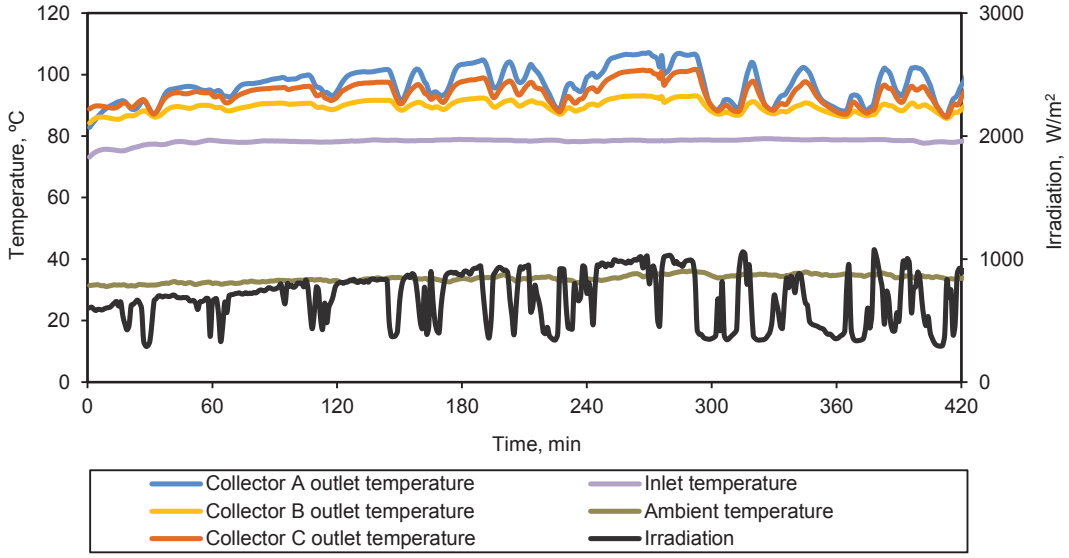

Fig. 3: Solar thermal collector performance for maintaining of the inlet water temperature of each collector at ~80°C. Collector outlet water temperatures, irradiation and ambient air temperature are shown in the figure. Caveat: "0 minute" considers the starting time of the experiments measurement. This time is generally between 9:30 to 10:00 a.m.

Since aperture area and water flow of each collector are different, the collector thermal performance could not be compared with this data alone. Therefore, collectors yield energy, i.e., thermal energy gain per unit collector aperture area has been analysed, as shown in Fig. 4.

As observed from Fig. 4, thermal energy gain per unit aperture area is different for each collector. Collector A is more responsive to the fluctuating irradiation followed by Collector B and Collector C. Collectors' materials properties and heat transfer mechanism of each collector attributes the difference of thermal energy gain of each collector. This comparison study provides the required data to consider the appropriate collector for industrial solar heating application in the tropics.

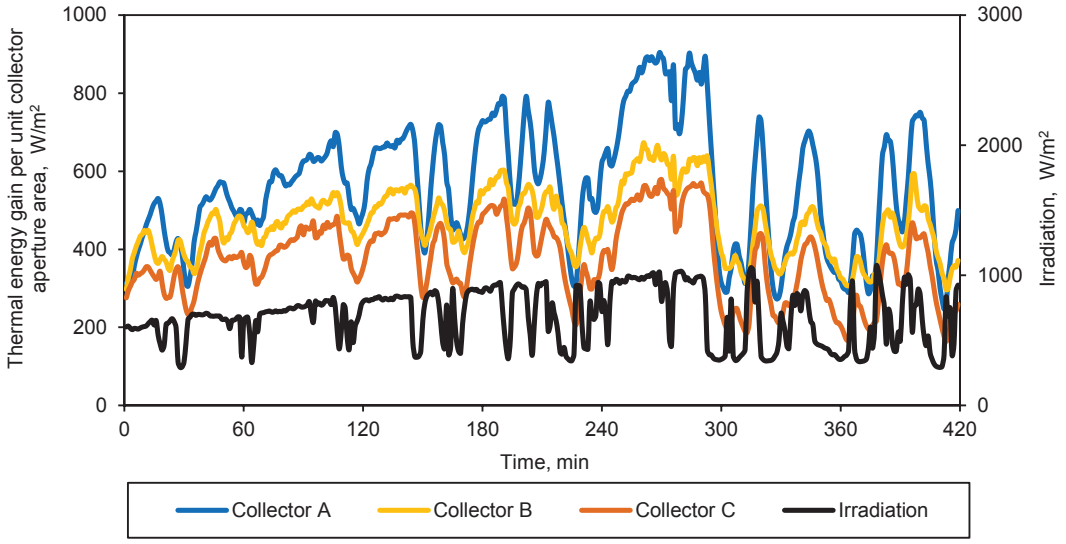

Fig. 4: Solar thermal collector thermal energy per unit collector aperture area when each collector inlet water temperature was maintained at ~80°C. Collector thermal energy gain per unit collector aperture area and irradiation are shown in the figure.
Caveat: "0 minute" considers the starting time of the experiments measurement. This time is generally between 9:30 to 10:00 a.m.

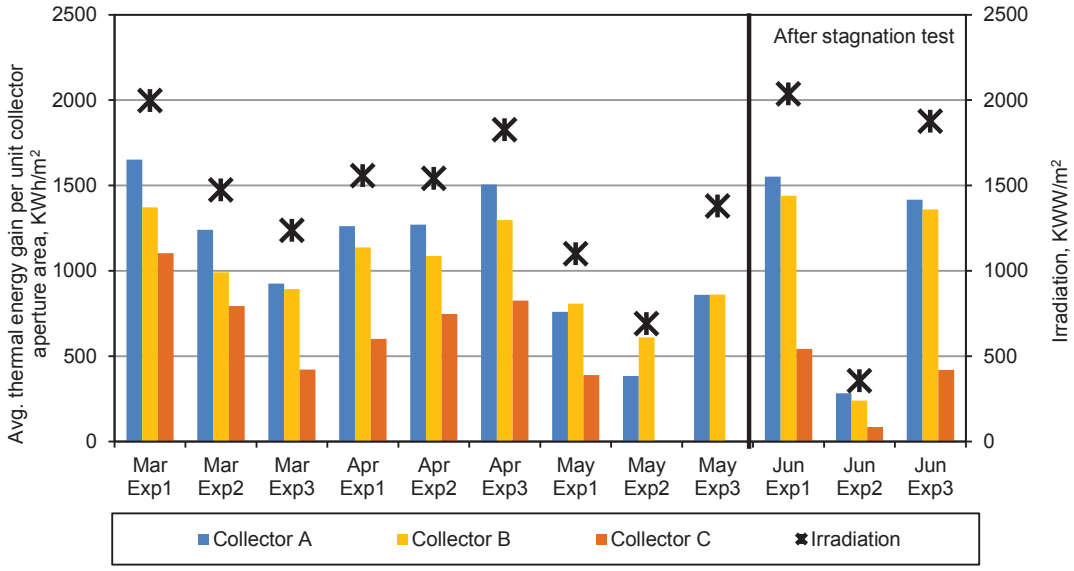

Fig. 5: Tested solar thermal collector thermal energy gain per unit collector aperture area when each collector inlet water temperature was maintained at 80°C (Exp1), 90°C (Exp2), 100°C (Exp3) on the month of March, April, May and June. June experiments were conducted after the stagnation test. Operating conditions of these experiments are given in Tab.2.
Caveat: Due to to technical failure some expermient results could not be recorded properly. Therefore, those data were not considered for analysis.

4.2. Outdoor test performance

Solar yield performance of the three collectors were analysed based on the experimental results. Average solar thermal gain for each month has been considered for this analysis. In the later part, collector efficiency parameters are compared on a monthly basis.

Yield energy

According to EN 12975 standard, the best way to compare different types of collectors is to compare the useful energy from a square meter of collector under equivalent circumstances (Standard 12975). Even though the present experiments of the three different types of collectors would not comply with the procedures of the mentioned standard, thermal energy gain per unit aperture area of each collector has been calculated for analysis purposes.

Fig.5 presents the comparison of thermal energy gain per unit collector aperture area among the three collectors under different operating conditions. As defined, the thermal energy gain by the collector depends on two factors – collector water temperature rise (delta T) and collector flow. Collector water temperature rise (delta T) is attributed to the solar irradiation absorbed and the collector heat losses. In the experiments, collector minimum flow according to manufacturer was attained for maximum temperature gain across the collector (highest delta T). It is observed from Fig.5 that the performance of the collector A and Collector B was the significantly higher than Collector C thermal performance under those boundary conditions. The difference of the collector performance would be due to the difference of technologies of heat gain and heat losses of these collectors. After stagnation test, Collector C performance was decreased significantly. Thus, the experimental findings would provide yield performance of the collectors before and after the stagnation test. But, these results would not be sufficient for comparison of the collector performance. For this reason, collector efficiency parameters had been analysed in the later sections.

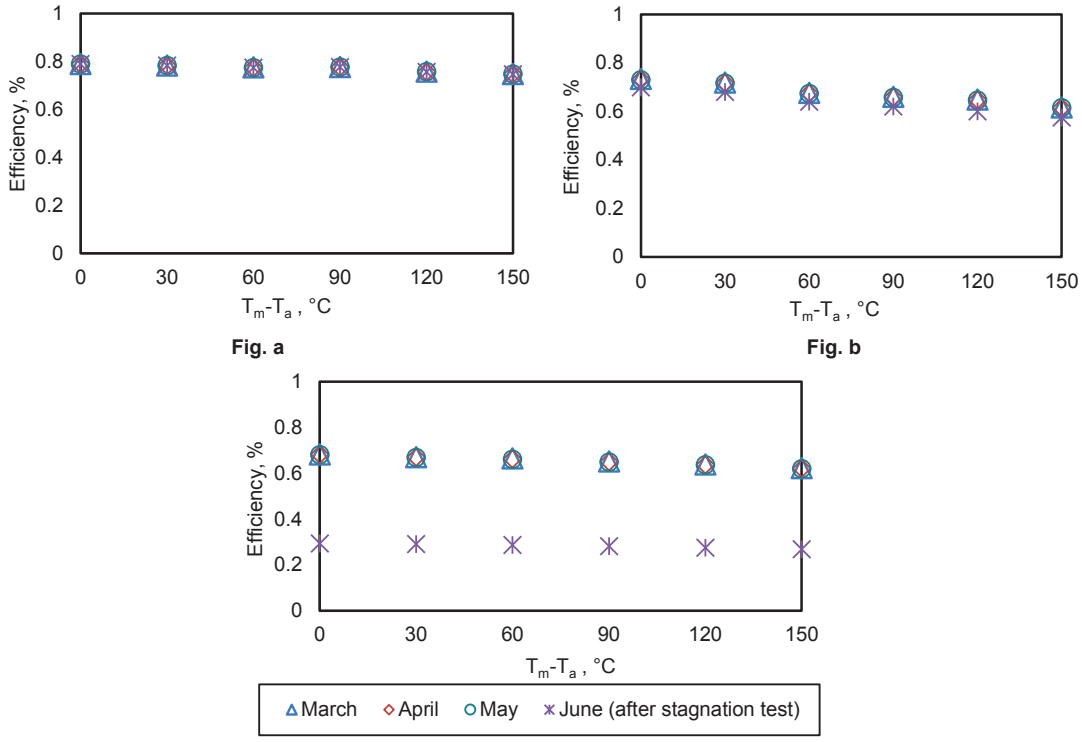

Fig. a **Fig. b** **Fig. c**

Fig. 6: Comparison of η vs (T_m-T_a) curve for unit aperture area and solar irradiance (G = 1000 W/m^2) values for testing months (March, April, May and June) of the collectors – Collector A (Fig. a), Collector B (Fig. b) and Collector C (Fig. c). June results present the collectors performance after the stagnation test.

Collector efficiency

The solar thermal collector models were validated with the experimental results, as discussed in section 3. In order to validate the collector models, the comparison of the collector outlet temperature between experimental and simulated values for the three different collectors were performed. The root mean square error (RMSE) of

the collector outlet temperature values between the simulated models and the experiments were found RMSE≤ 1K, which is not significant. The validated collector models, as presented in Section 3.3, were used to determine the efficiency parameters η_0, a, and b of the stationary model from (eq. 6). Applying the least squares approach, the coefficients η_0, a and b were determined for analysis of collectors performance

Fig.6 shows the calculated collector efficiency of the three different collectors for the temperature difference ($T_m - T_a$) when solar irradiance G=1000 W/m^2 on the collector plane. The efficiency functions are a result of a least square fit of the simulated values with a second order polynomial. This efficiency functions takes into account that the heat loss coefficient of the collectors is a function of temperature.

Comparison of the Collector A efficiency, as shown in the Fig. 6(a), revealed no degradation of the collector performance during testing from March to May. Even after the stagnation test on June, Collector A performance degradation has not been observed.

Comparison of the Collector B efficiency, as shown in the Fig. 6(b), revealed no degradation of the collector performance during the actual testing from March to May. After the stagnation test, a small order of degradation of the collector performance has been observed. After stagnation test, no defects were noted from outer inspection during collector operation. Thus, it might suspect that the collector materials, presumably the absorbent layer, could have degraded due to the high temperature of the stagnation test.

Comparison of the Collector C efficiency, as shown in the Fig. 6(c), revealed that here was a significant degradation of the performance after stagnation test. In this collector field, there are heat pipes which could be damaged and/or spoiled due to the excess heat during stagnation test. Because of this, the Collector C performance degraded after stagnation test.

Though the analyses of these collectors provide an insight of the collector performances for the given duration of the outdoor testing in Singapore, degradation of the collector performances for a longer period of operation could not be determined from these analyses.

5. Summary

This paper describes a test methodology for comparing collector performance in tropical climatic conditions like Singapore. An outdoor test facility has been setup at the roof top of SERIS facility, where different collectors performance can be tested side-by-side for different operating conditions. Experimentally measured data is used to validate the collector dynamic model. The model is then utilized to identify the collector efficiency parameters.

In this paper, three different collectors- Collector A, Collector B and Collector C were studied. Based on the experiments and simulation results of the three collectors, the following findings can be summarized:

- Solar thermal yield (energy performance) of the Collector A and the Collector B are higher than the solar yield (energy performance) of the Collector C.
- There was no degradation of the Collector A, Collector B and Collector C performance was observed during first three months of outdoor testing (before stagnation test). The reason is that three months outdoor testing would not enough duration to observe any collector performance degradation.
- After the stagnation test, no degrading of the Collector A had been noticed. The Collector B performance showed some degradation of collector performance, while the Collector C showed a considerable performance degradation.

Performance analyses of the three different collector show that the Collector A and Collector B could consider for industrial heating applications in Singapore.

Finally, the present analysis of the collector performances for outdoor testing in Singapore provides a valuable basis for the selection of the relevant collector technologies for a large-scale solar thermal systems. Other factors such as, relevant costs associated with the collector (including installation and maintenance costs) and the long-term durability have to be considered though in order to design, implement and operate a large scale solar thermal installation.

6. Acknowledgement

The work is supported by a project with a multinational pharmaceutical company.

7. References

Amer, E.H., Nayak, J.K., Sharma, G.K., 1997. Transient test methods for flat-plate collectors: review and experimental evaluation. Sol. Energy 60 (5), 229–243.

Deacon, E.L., 1970. The derivation of Swinbank's long-wave radiation formula. Q.J.R.Meterol.S. 96(408); 313-319.

IEA SHC Task 49, The Solar Heat for Industrial Processes – SHIP online database contains a worldwide overview on existing solar thermal plants for different industry sectors. < http://ship-plants.info/>, !8 September, 2016.

Kong, W.Q., Wang, Z.F., et al., 2012a. Theoretical analysis and experimental verification of a new dynamic test method for solar collectors. Sol. Energy 86 (1), 398–406.

Kong, W.Q., Wang, Z.F., et al., 2012b. An improved dynamic test method for solar collectors. Sol. Energy 86 (6), 1838–1848.

Kratzenberg, M.G., Beyer, H.G., Colle, S., 2006. Uncertainty calculation applied to different regression methods in the quasi-dynamic collector test. Sol. Energy 80 (11), 1453–1462.

Material properties <www.engineeringtoolbox.com>; DOI: 30 August, 2015.

Mahbubul, M., 2013.Optimization of solar thermal collector systems for the tropics, M.S. Thesis, National University of Singapore.

Praëne, J.P. , Garde, F., et al., 2005. Dynamic modelling and elements of validation of a solar evacuated tube collector, Building Simulation, 953-960.

Perers, B., 1997. An improved dynamic solar collector test method for determination of non-linear optical and thermal characteristics with multiple regression. Sol. Energy 59 (4-6), 163–178.

Xu, L., Wang, Z.F., et al., 2012. A new dynamic test method for thermal performance of all-glass evacuated solar air collectors. Sol. Energy 86 (5), 1222–1231.

Quality assurance in solar heating and cooling technology. A guide to the standard EN12975 <www.estif.org/fileadmin/estif/content/projects/QAiST/QAiST_results/QAiST%20D2.3%20Guide%20to%20EN%2012975.pdf> DOI: 18 September, 2016.

Appendix: **UNITS AND SYMBOLS**

Table 1: Symbols and units

Quantity	Symbol	Unit
Area	A	m^2
Global heat loss coefficient	a	$W\ m^{-1}\ K^{-1}$
Temperature dependent of global heat loss coefficient	b	$W\ m^{-2}\ K^{-2}$
Specific heat	c	$J\ kg^{-1}\ K^{-1}$
Diameter	d	m
Global irradiance	G	$W\ m^{-2}$
Heat transfer coefficient	h	$W\ m^{-2}\ K^{-1}$
Heat capacity	J	$J\ m\ kg^{-1}.K^{-1}$
Mass flow rate	$\dot{m}$	$kg\ s^{-1}$
Temperature	T	K or °C
Velocity	u	$m\ s^{-1}$
Absorptance	α	
Emittance	ε	
Density	ρ	$kg\ m^{-3}$
Transmittance	τ	
Efficiency	η	
Stefan-Boltzmann constant	σ	$W\ m^{-2}\ K^{-4}$

Table 2: Subscripts

Quantity	Symbol
Ambient	a
Absorber	c
Fluid (water)	f
Glass	g
Inlet	i
nner	in
Outlet	o
Optical	o
Mean	m
Sky	sky